THE ASTROPHYSICAL JOURNAL, 382:301–314, 1991 November 20

ON THE WIND GEOMETRY OF THE WOLF-RAYET STAR EZ CANIS MAJORIS

R. E. SCHULTE-LADBECK, K. H. NORDSIECK, M. TAYLOR, M. A. NOOK,[1] K. S. BJORKMAN, A. M. MAGALHÃES, AND C. M. ANDERSON
Space Astronomy Laboratory, University of Wisconsin at Madison, 1150 University Avenue, Madison, WI 53706
Received 1991 February 22; accepted 1991 May 20

ABSTRACT

Recent models of Wolf-Rayet star winds have been tailored to EZ CMa, and make predictions of the envelope structure and location of line-emitting regions. We discuss how the wind structure of EZ CMa can be probed observationally through electron distribution integrals as measued by spectropolarimetry, and then present, analyze, and interpret a time-dependent spectropolarimetric data set of EZ CMa. The observations further our view of an electron-scattering wind that is axisymmetric, rotating, and expanding, with a variable mass-loss rate being responsible for the quasi-periodic polarimetric variability. We demonstrate that the emission lines of EZ CMa are partially polarized, indicating that line photons are electron-scattered in the wind. The polarization in N V λ4945 and N IV λ4058 is observed to be larger than that of He II λ4686 and He I λ5876, as expected from ionization stratification.

Subject headings: polarization — stars: individual (EZ Canis Majoris) — stars: winds — stars: Wolf-Rayet

1. INTRODUCTION

It was realized by Beals (1929) that the extended atmospheres of Wolf-Rayet (W-R) stars are responsible for the prominence of broad and strong emission lines in their spectra. Because of these dense stellar winds, the hydrostatic surfaces of W-R stars are not accessible to direct observation; in fact, the continua themselves are formed in a geometrically extended region (Cassinelli & Castor 1973). The emission-line–dominated W-R spectra were not approachable by quantitative analysis for a long time, since model calculations for static, plane-parallel stellar atmospheres are not adequate. Hence, basic stellar parameters such as radii, temperatures, and luminosities as well as atmospheric conditions were elusive.

This situation improved recently when elaborate computer codes for non–LTE radiation transfer in expanding atmospheres were developed by Hillier (e.g., 1987a, b, 1988) and Hamann, Schmutz, & Wessolowski (1988). In these spherically symmetric, homogeneous, and stationary empirical models the temperature, radius, and mass loss of the star are treated as parameters and matched to the spectral energy distribution, line strengths, and profiles. The W-R star EZ CMa = HD 50896 = WR 6 has come to play a key role in the study of W-R stars, since it has been chosen as the prototype WN5 star for both sets of models. It is a firm prediction of both models that the ionization in the wind of EZ CMa decreases outward. The variable ionization structure has important implications for line formation in the stellar wind, with, e.g., the He I recombination lines arising at larger radii than those of He II. Hillier (1987a) illustrated that the continuum-forming region becomes more extended as a function of increasing wavelength and that the continuum energy distribution in the optical and IR is controlled primarily by the density in the wind, while it is relatively insensitive to the luminosity of the underlying star.

The new models reveal that the mass loss has a profound effect on the spatial structure of the envelope. In order to test the models, one would like to obtain direct observational measures of the star/wind geometry. Polarimetry is such a measurement, and is the concern of this paper.

[1] Now at Department of Physics and Astronomy, St. Cloud State University, St. Cloud, MN 56301.

1.1. *The Polarimetric Technique*

The wind around EZ CMa is highly ionized, thus containing liberal amounts of free electrons. When photons interact with these electrons, they are scattered. If the object were resolved, the degree of polarization could be as high as 100%, i.e., for pure, single-electron scattering viewed at a scattering angle of 90°; because it is not resolved, the polarization integrated over the envelope must cancel unless the geometry is not spherically symmetric. It is well documented (see below) that the light from EZ CMa is polarized. Since the direct, unscattered starlight is included in the beam as well, the observed polarization is much reduced to values on the order of a few tenths of a percent of the intensity. Spectropolarimetry is therefore a difficult measurement and has not been widely used to investigate W-R stars.

A simple case of nonspherical geometry is axial symmetry. The residual polarization of an optically thin electron envelope with axial symmetry centered on the star but with otherwise general density distribution and an arbitrary inclination i can be expressed as

$$P_R \approx 2\bar{\tau}(1 - 3\gamma) \sin^2 i \,, \tag{1}$$

where $\bar{\tau}$ is the mean Thomson scattering optical depth of the envelope:

$$\bar{\tau} = \frac{3}{32} \sigma_T \int_{r=0}^{\infty} \int_{\mu=-1}^{1} n_e(r, \mu) dr \, d\mu \,. \tag{2}$$

Here σ_T is the Thomson cross section, $n_e(r, \mu)$ is the electron density (where μ has been substituted for cos Θ, while Θ is the angle between the symmetry axis and the scatterer located at a distance r from the [point-source] star), and γ is a shape factor defined by the ratio of two integrals of the density distribution measuring the flattening of the envelope (Brown & McLean 1977). The *amount of polarization* thus contains information on the geometric shape or density distribution of the circumstellar material. The electron-scattering cross section is independent of wavelength and produces a flat polarization spectrum.

Cassinelli & Hummer (1971) showed that by assuming a point-source star the polarization of an extended envelope is overestimated because the radiation field from a point is

always forward-peaked. Cassinelli, Nordsieck, & Murison (1987) reformulated the problem by including a finite source, called the "finite-disk" factor, in the integrals over the density distribution of an axisymmetric electron envelope (neglecting for simplification the occultation of electrons behind the star). In W-R stars, the "finite-disk" factor might not be a constant but should increase with wavelength as the radius of the continuum-forming region increases with wavelength. We may thus expect the polarization to decrease from the UV to the IR, and henceforth obtain new envelope diagnostics from the *color of polarization.*

The wavelength dependence of the continuum polarization may be modified by absorption and emission processes in the wind. Cassinelli et al. (1987) calculated the polarization from a hydrogen plume in the wind of an O star, including single-electron scattering and optically thin absorption (but no reemission). The color of the polarization depends on the square of the electron density because the populations of the excited levels of hydrogen are proportional to n_e^2. A similar process could work in W-R stars. Bound-free and free-free effects should even be more important in W-R stars than in O stars because of the higher wind densities. The plume model can be adapted to W-R stars by substituting the He bound-free opacities for the H opacity in the plume, and, since the opacities of He II and H I have very similar (λ^3) wavelength dependencies, we may even expect the continuum polarization to rise into the UV in a way similar to the hydrogen plume model. In the plume model, the strength of the (polarization) Balmer jump is a strong function of temperature; the jump becomes smaller as the temperature increases because less of the hydrogen in the plume is neutral. The winds of W-R stars are highly ionized. There is usually either no change in flux across the He II (n–4) edge, or the jump is seen in emission in strong-line WN stars, e.g., in EZ CMa (see Schmutz 1991). Dilution by unpolarized bound-free continuum emission within the wind must thus be accounted for as well in determining the color of the polarization. The dilution at the continuum discontinuities should be small, since the jumps are not very strong flux features. A more important contribution might result from dilution by free-free emission. The free-free opacity of a hydrogenic ion has a λ^3 wavelength dependence and scales with n_e^2.

Similarly, the polarization may become modulated through line opacities. Recombination produces unpolarized emission lines, and the continuum polarization is reduced at the line wavelength (see also eq. [20]). However, if the line photons are subsequently scattered, they became polarized. The total *line polarization* hence carries information on the envelope stratification, and we may obtain insight into the radial distribution of material.

Last, a line might itself be polarized as a result of the excitation mechanism. This is the case for resonance fluorescent scattering. The line polarization becomes an indicator of the line formation process.

Whereas we have considered a static system up to now, if either the geometry, the electron density, or the aspect angle varies as a function of time, additional information is contained in the *time dependence of polarization.* This aspect is important in the case of EZ CMa, because it has repeatedly been claimed to be a binary system (see, e.g., Firmani et al. 1980). Brown, McLean, & Emslie (1978) have discussed the polarization arising in an envelope of arbitrary electron distribution illuminated by any number of point sources with the special application to phase-locked polarization in binaries. They obtain six integrals for the optical depths and shape factors, representing the electron-scattering optical depth integrated over all directions, the shape factor for flattening similar to the one in equation (1), the effective degree of asymmetry about the orbital plane (first harmonic variations in the polarization time dependence), and the effective concentration of material in the orbital plane (second harmonic variability). Both the direction and the amount of polarization are thus variable. We note that periodic polarization variations may just as well occur from a single star surrounded by a nonspherical, inhomogeneous, rotating envelope or a processing disk.

1.2. *Previous Results on EZ CMa*

Intrinsic polarization in EZ CMa was discovered by Serkowski (1970) through measurements of the linear polarization as a function of time. This implies immediately a sufficient scattering optical depth and a nonspherically symmetric geometry/density distribution. For an axisymmetric envelope it indicates a non–pole-on aspect ($i \neq 0$) or time-dependent inhomogeneities in the electron distribution if $i = 0$. Serkowski found that the polarization in the ultraviolet was larger than in the blue and yellow, in contrast to his observations of OB supergiants, and that there was no correlation between polarization and brightness.

A measurement of the wavelength dependence of the linear polarization was obtained by McLean et al. (1979). Their data consist of a true spectropolarimetric data set covering the wavelength range from 3400 to 6000 Å at a spectral resolution of 50 Å obtained in 1977 November, and a set of eight narrow-band (50 Å) filter measurements obtained in the winter of 1978. The polarization across the emission lines of He I, He II, N IV, and N V decreased with respect to the continuum. The latter was flat and suggestive of electron scattering. The polarization at the lines was reported to be consistent with unpolarized emission for most lines, and recombination as the likely emission mechanism. He II λ4686 showed a polarization well above the average curve, and He I λ5876 was less polarized than predicted; this was interpreted as evidence for stratification and for an outward decrease in ionization. Because of the absence of polarization changes across the Balmer jump, a high degree of ionization and/or hydrogen deficiency of the envelope was suggested. The intrinsic position angle of the polarization was found to be independent of wavelength, even across the lines. However, the position angle did change with time between the two epochs, which was considered to indicate a nonaxisymmetric geometry. But, since the polarization was observed to be rather large, $\sim$1.5%, some flattening or localization of the envelope was required nevertheless, which could not coincide with the line of sight to Earth. In addition, the polarization was noted to have changed substantially over the course of only a few hours in the Serkowski data set, and the authors suggested that this could be linked to changes in electron density on the order of 10% in the mass loss (e.g., owing to clumpiness) or to variable absorption in a gas stream.

Firmani et al. (1980) reported the discovery of photometric and spectroscopic changes with a period of 3.76 days and proposed that EZ CMa is a binary in which the WN5 star has a neutron star companion. Subsequently, McLean (1980) monitored the time dependence of the linear polarization over a 4 month interval starting in 1979 January, mostly in the *B* filter (effective wavelength $\sim$4250 Å). He indeed detected phased-locked polarization variation with a peak-to-peak amplitude

of 0.3% or higher in each Stokes parameter. The dominant variation was found to be in the second harmonic, as is expected from a binary system. McLean pointed out that, in addition to this small periodic component, there was also a large static component in the data (assuming the same interstellar polarization used in McLean et al. 1979); thus the major part of the polarization was thought to be the manifestation of an oblate envelope structure with symmetry about the stellar rotation axis. He identified four potential sources for the periodically variable polarization component, namely, nonradial pulsations, hot-spot rotation, binarity, or some other mechanism, such as magnetic fields. Nonradial pulsations combined with rotation were considered a good possibility. Rotation of a hot spot, because of the fact that the spot would get eclipsed, should produce first harmonic variations, and was ruled out. Polarization of magnetic origin was tentatively ruled out because of the lack of circular polarization reported by McLean et al. (1979), a result recently confirmed by Drissen et al. (1989). It was concluded that the periodic polarization component was most consistent with a binary model, yielding then an orbital inclination of 71° from the polarimetry, in good agreement with the deductions of Firmani et al. (1980). However, McLean also indicated the occurrence of additional nonperiodic variability in his data, attributable to a stochastic process in the W-R star envelope.

Drissen et al. (1989) presented a large photo-polarimetric data set obtained in 1985 September and 1986 October. Variability was found to be consistent with a 3.77 day period. The polarimetric behavior was coherent within a 2 week interval, but was variable on a time scale of months. The 1986 data were described reasonably well with an eccentric binary model, whereas the other data were not. Drissen et al. suggested two explanations, namely, either that the data have nothing to do with binary modulation, the observed phenomenon being fortuitously similar to the binary model, or that the binary modulation is always present in conjunction with another phenomenon. As a nonbinary option, the presence of a rotating, semistable bright spot somewhere in the W-R envelope was explored and found to give a possible explanation of both the polarimetric (in the case of multiple spots) and the photometric behavior. This hypothesis was not favored because of time-scale considerations, the replacement time in the wind being on the order of hours, and the requirement of an unknown confinement mechanism for such a long-lived spot or eddy.

A combined spectroscopic, photometric, and polarimetric data set for the observing seasons 1988–1990 was gathered by Robert et al. (1991). A 3.766 day period again occurred in the polarimetry, while the photometry displayed three minima per 3.766 day cycle, and the spectroscopy revealed no clear periodicity in the line-profile variations. Three options were discussed, a rotating star with spots, pulsations, and duplicity, but none proved to be satisfactory.

Schulte-Ladbeck et al. (1990, hereafter Paper I) reported the discovery through spectropolarimetry of linear polarization changes across the profile of the line He II λ4686. They proposed that the continuum polarization in EZ CMa can be understood by an electron-scattering, axisymmetric, rotating and expanding envelope inclined to the line of sight, with the decrease in polarization in He II being caused by increased absorptive opacity in the line and dilution by unpolarized line emission, while the variations in position angle are due to Doppler-shifted absorptive opacity and/or scattered line photons. A single-star model was favored, since the sense of polarization rotation in the line was independent of phase, and the overall polarization varied with the first harmonic.

2. INSTRUMENTATION AND OBSERVATIONS

The data were obtained with the medium-resolution, high-throughput, dual-beam spectropolarimeter on the 0.9 m telescope of the Pine Bluff Observatory of the University of Wisconsin. The instrument measures the three Stokes parameters Q, U, and I simultaneously over the spectral range from $\sim$3200 to 7800 Å. The polarization optics and the camera used for observations in 1990 were designed by Nordsieck (1987, 1991). A Boller & Chivens small-telescope spectrograph was heavily modified by inserting a rotating achromatic quartz and magnesium fluoride half-wave plate after the slit and a large-aperture calcite Wollaston beam splitter in the collimated beam just before the grating. For all observations reported here, a grating with a dispersion of 300 lines mm^{-1} which yields 5 Å $pixel^{-1}$ was used. This provides a spectral resolution of $\sim$34 Å FWHM with the 12 arcsec^2 entrance aperture. The camera feeds a proximity-focused microchannel-plate intensifier coupled to a pair of 1024S Reticon arrays mounted side by side on the same substrate. The two Reticon arrays detect the two spectra of orthogonal polarization split by the Wollaston prism. Therefore, the observing method is differential and not prone to scintillation variations; object-sky switching is used to cancel atmospheric transparency variability. Two internal lamps are used for flat-field and wavelength-calibration observations.

The wave plate is rotated in steps of 11°.25 and is oriented so that observations in the initial position measure the Q parameter. The polarization is observed at eight orientations of the wave plate, and the Stokes parameters are calculated from Fourier analysis. A total of 32 observing cycles, sky-star-star-sky through the eight plane positions, constitutes one polarimetric measurement. The reduction program provides the least squares of the Fourier fit for each measurement, so that data subsets with large chi-squares (i.e., due to transparency variations with a frequency larger than the polarimetric modulation of the signal) can be rejected in the reduction.

The instrument is mounted on a dedicated telescope and operated every clear night. The observing program is designed to accommodate this mode, e.g., standard stars need to be observed less frequently, and the nightly observer selects a program object from a general observing list updated once a week instead of carrying out an "observing run."

We usually observe three flux standards every night. But, given the quality of the site, the photometric calibration is hardly ever absolute. By using a 12 arcsec^2 aperture for all observations, it is ensured that the entire stellar image passes to the spectrograph. The colors with this aperture have been analyzed by Nook (1990) using observations of about 50 flux standards observed over an interval of 5 months. The colors were found to be good to within 0.05 mag.

The polarimetric stability of the system is monitored by observing unpolarized and highly polarized standard stars roughly once a week. The polarimetric calibration of the instrument was determined from observations of bright stars through a Polaroid filter, and of unpolarized and highly polarized standard stars.

An all-refractive-element camera designed by K. Nordsieck was used for the observations in 1990. Using a baseline of

several months, we have determined that the instrumental stability is 0.005% or better, and the nightly error in the polarimetric efficiency is smaller than 1 part in 100. Therefore, our systematic errors should be smaller than 0.01%. A journal of observations is given in Table 1 of Paper I.

Before 1990 January, we used the original achromatic Maksutov camera that was supplied with the spectrograph. This camera caused some vignettting and reduced the polarimetric stability to 0.11%. Our pilot data for this project were obtained on 1989 March 8 with this camera. We include the data for qualitative comparisons with the 1990 data.

3. RESULTS AND INTERPRETATION

The results of the spectropolarimetric observations are displayed in Figure 1 and are labeled with the data of observation. The top panels show the flux spectrum; the two lower panels are the percentage polarization and the position angle with respect to the equatorial plane. The reduction software allows for error-dependent binning. To facilitate the comparison between nights, the polarimetric error was set to be the same, 0.08%, for each night. Thus the polarimetric data show variations in resolution across the spectrum which reflect the count rates recorded at that wavelength.

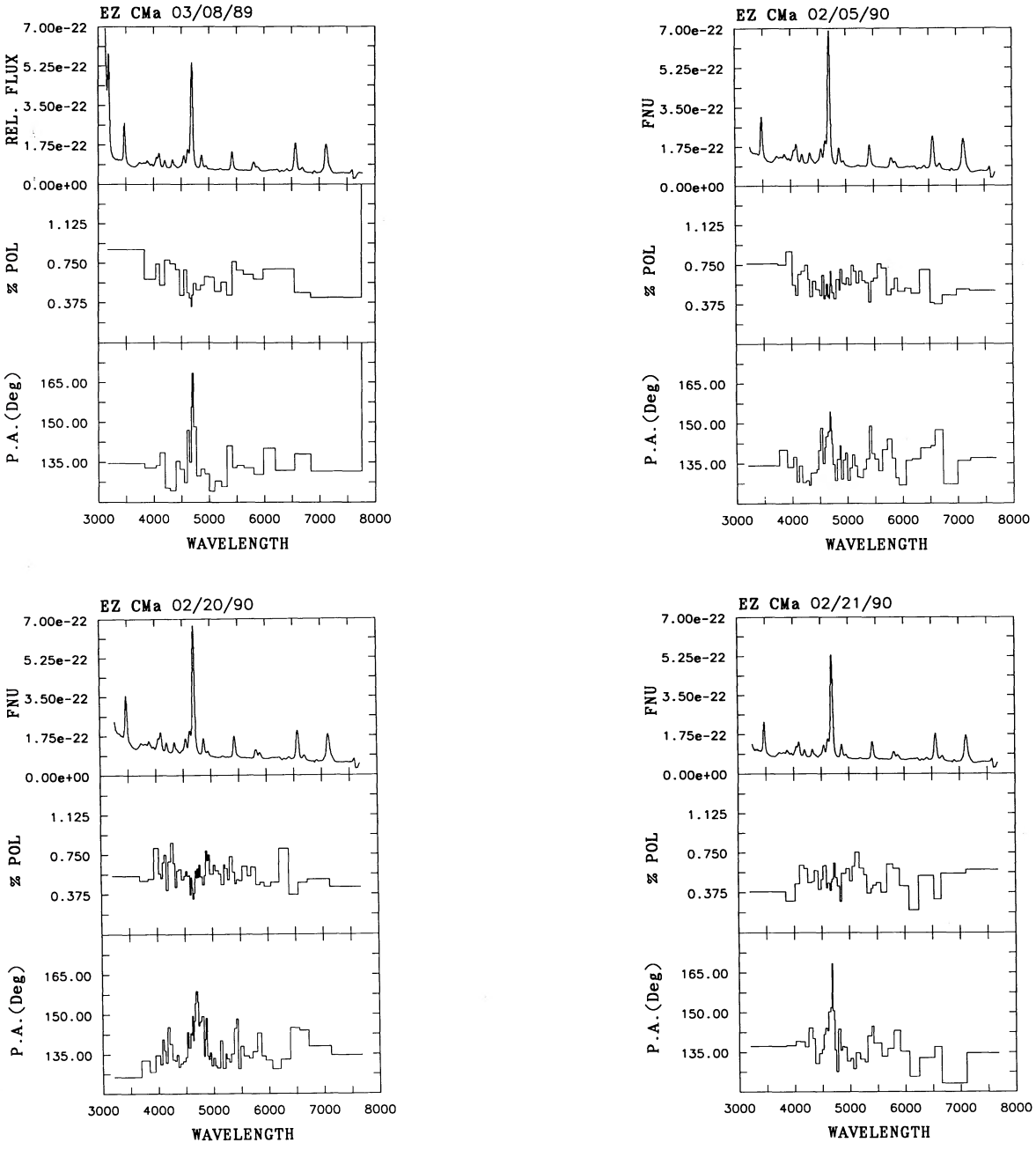

FIG. 1.—Observed spectropolarimetry of EZ CMa. The flux in ergs cm^{-2} s^{-1} Hz^{-1}, degree of linear polarization in percent, and equatorial position angle in degrees are plotted as a function of wavelength in angstroms. The date of observations is indicated at the top of each plot.

Because different conventions are used in the literature, we wish to give a definition of the terminology employed throughout this paper. The linear polarization Stokes parameters are

$$Q^I = P_L I \cos(2\Theta), \quad (3)$$

$$U^I = P_L I \sin(2\Theta), \quad (4)$$

where P_L is the degree of linear polarization, I is the intensity, and Θ is the position angle. We will refer to Q^I and U^I as polarized intensities. Our measurements are usually expressed in intensity-normalized Stokes parameters,

$$Q = 100Q^I/I = P \cos(2\Theta), \quad (5)$$

$$U = 100U^I/I = P \sin(2\Theta), \quad (6)$$

where P is given by

$$P = 100P_L = (Q^2 + U^2)^{1/2} \quad (7)$$

and the position angle is given by

$$\Theta = \tfrac{1}{2} \tan^{-1}(U/Q) \quad (8)$$

with respect to the equatorial coordinate system. We will normally give Q and U, as well as P, in percent and refer to them as the percentage polarization.

The observed polarization of EZ CMa will be composed of two quantities, the intrinsic polarization formed in the star/envelope and the interstellar polarization added by passage of the light through aligned dust grains in the interstellar

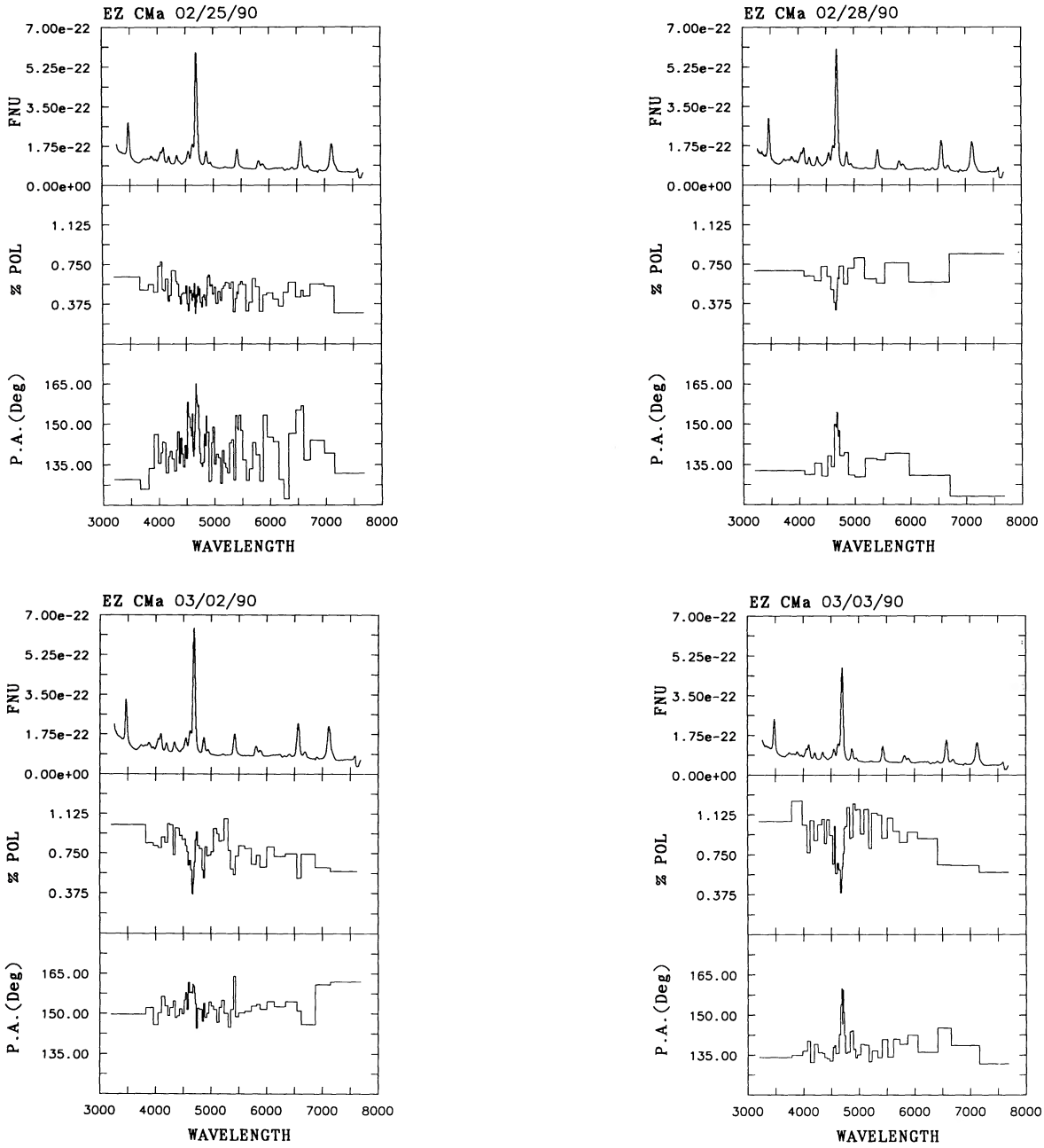

FIG. 1—*Continued*

medium. The amount, position angle, and wavelength dependence of the interstellar polarization are constant with time. However, unlike "reddening," which is a scalar with well-determined properties added to the intensity, interstellar polarization is a vector, and only the shape of its wavelength dependence is a descriptive, average property. If both the interstellar polarization and the intrinsic polarization are small, the observed polarization is a superposition that can be written as

$$Q_{\text{observed}}(\lambda, t) = Q_{\text{interstellar}}(\lambda) + Q_{\text{intrinsic}}(\lambda, t)\,, \quad (9)$$

$$U_{\text{observed}}(\lambda, t) = U_{\text{interstellar}}(\lambda) + U_{\text{intrinsic}}(\lambda, t)\,. \quad (10)$$

It is usually a difficult problem to remove the interstellar polarization and determine the intrinsic polarization of an object. However, there are many conclusions that can be drawn from the observed polarization alone, particularly through its time dependence. We will therefore analyze the observed polarization in EZ CMa first, and will attempt to remove the interstellar polarization later in the paper.

3.1. *Inferences from the Observed Polarization*

From visual inspection of Figure 1, we can immediately draw a number of conclusions. Both the polarization and the position angle change at the wavelengths of emission lines as compared with the adjacent continuum levels. The 1990 data cover a full range of phases throughout the 3.7 day period (refer to Table 1 of Paper I). The polarization changes are seen at all times. These polarization changes are a persistent phenomenon in EZ CMa, since they were present in McLean's 1978 and 1979 data, in our 1989 data set, and in all of the 1990 data. They indicate that the light from EZ CMa was intrinsically polarized at all these times.

The continuum levels of the observed polarization and position angle are variable. The polarization varied little during five nights in 1990 February but changed drastically during two consecutive observing nights in March. We can infer from both the wavelength and the time dependence of the polarization that part of the observed polarization is intrinsic to EZ CMa and that the intrinsic polarization is not transient. If we could assume that the emission lines themselves are completely unpolarized, they would give us the amount and direction of the interstellar polarization. While the line polarization has yet to be analyzed in more detail, it is apparent that the temporal polarization changes are most pronounced to continuum photons.

If we integrate the polarization over the entire spectrum, the total amplitude of the variations observed in 1990 is $\sim$0.4%. At least this amount of polarization is then intrinsic to the star, and indicates a large electron density distribution integral toward the line of sight. The variability amounts to either profound changes in the electron density, geometry, or changes in the aspect as seen from Earth. The integrated polarization represents a wide-filter observation. We have plotted the 1990 data as a function of phase using the ephemerides of Lamontagne, Moffat, & Lamarre (1986). The phase dependence is illustrated in Figure 2, and can be compared with the filter observations obtained in the spring of 1990 by Robert et al. (1991). In the 1990 observing season, all observations showed only one pronounced polarization peak around phase 0.8–0.9. Binary modulation usually produces two phase peaks in the polarization.

The change of polarization at the emission-line wavelengths modifies the polarization very strongly. For the strongest line,

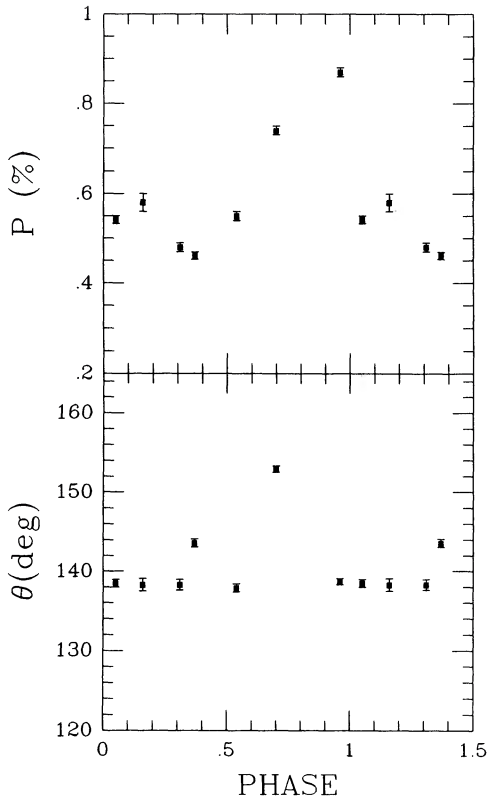

FIG. 2.—Integrated polarization vs. phase

He II λ4686, it is also apparent that its strength, i.e., line-peak–to–continuum flux ratio, varied with time, indicating a variable contribution of the line fluxes to the spectra. Wide-filter (polarimetric) observations are thus difficult to interpret, since they include the continuum and a wealth of emission lines. To separate out the continuum polarization in our data, we have defined six line-free spectropolarimetric filters, in analogy to the line-free spectrophotometric indices used in the literature for continuum photometry (e.g., Torres-Dodgen & Massey 1988). We have both considered the wavelength intervals used for spectrophotometry and also judged from our own spectroscopy regions that appear to be good continuum areas. An averaged spectrum of all 1990 data is displayed in Figure 3. In this figure we illustrate the continuum regions that have been chosen interactively. The definitions of our continuum filters are R = 3561–3711 Å, E = 4419–4467 Å, G = 5073–5175 Å, I = 5571–5733 Å, N = 5979–6063 Å, A = 7287–7515 Å. The polarizations measured in these filters are given in Table 1. In the two panels of Figure 4 we display the percentage polariza-

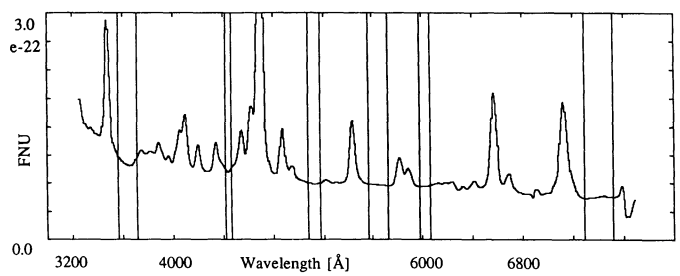

FIG. 3.—Selected "line-free" continuum bandpasses

TABLE 1

POLARIZATIONS WITH VARIOUS FILTERS

Filter	JD 2,447,900+	*P*	*dP*	P.A.	*d*P.A.	Filter	JD 2,447,900+	*P*	*dP*	P.A.	*d*P.A.
All	26.58	0.55 %	0.01 %	137°9	0°5	I	25.68	0.68 %	0.06 %	138°	2°
	42.66	0.542	0.009	138.5	0.5		42.66	0.62	0.05	133	2
	43.63	0.48	0.01	138.3	0.7		43.63	0.46	0.06	135	4
	47.61	0.461	0.008	143.6	0.5		47.61	0.42	0.05	137	3
	50.60	0.58	0.02	138.3	0.8		50.60	0.76	0.13	139	5
	52.62	0.74	0.01	152.9	0.4		52.62	0.76	0.07	149	3
	53.61	0.87	0.01	138.7	0.4		53.61	0.96	0.07	139	2
R	25.68	0.79	0.13	131	5	N	25.68	0.51	0.09	127	5
	42.66	0.48	0.10	126	6		42.66	0.47	0.09	130	5
	43.63	0.40	0.16	146	11		43.63	0.66	0.11	128	5
	47.61	0.58	0.10	123	5		47.61	0.55	0.09	146	5
	50.60	0.23	0.31	186	26		50.60	1.33	0.22	132	5
	52.62	1.18	0.14	151	3		52.62	0.76	0.11	155	4
	53.61	1.20	0.14	131	3		53.61	1.11	0.12	144	3
E	25.68	0.60	0.07	130	3	A	25.68	0.29	0.14	143	13
	42.66	0.58	0.07	131	3		42.66	0.38	0.19	123	13
	43.63	0.52	0.09	137	5		43.63	0.58	0.25	133	12
	47.61	0.49	0.06	137	3		47.61	0.23	0.16	121	17
	50.60	0.88	0.12	130	4		50.60	2.29	0.55	109	7
	52.62	1.02	0.09	148	2		52.62	0.54	0.18	163	9
	53.61	1.08	0.08	134	2		53.61	0.78	0.31	99	11
G	25.68	0.68	0.05	136	2	He II	25.68	0.50	0.03	152	2
	42.66	0.55	0.05	136	3		42.66	0.52	0.04	157	2
	43.63	0.71	0.06	132	3		43.63	0.50	0.07	160	4
	47.61	0.50	0.04	135	2		47.61	0.44	0.02	158	2
	50.60	0.70	0.11	129	4		50.60	0.54	0.04	148	2
	52.62	0.93	0.05	151	2		52.62	0.57	0.03	160	2
	53.61	1.14	0.07	141	2		53.61	0.54	0.04	155	2

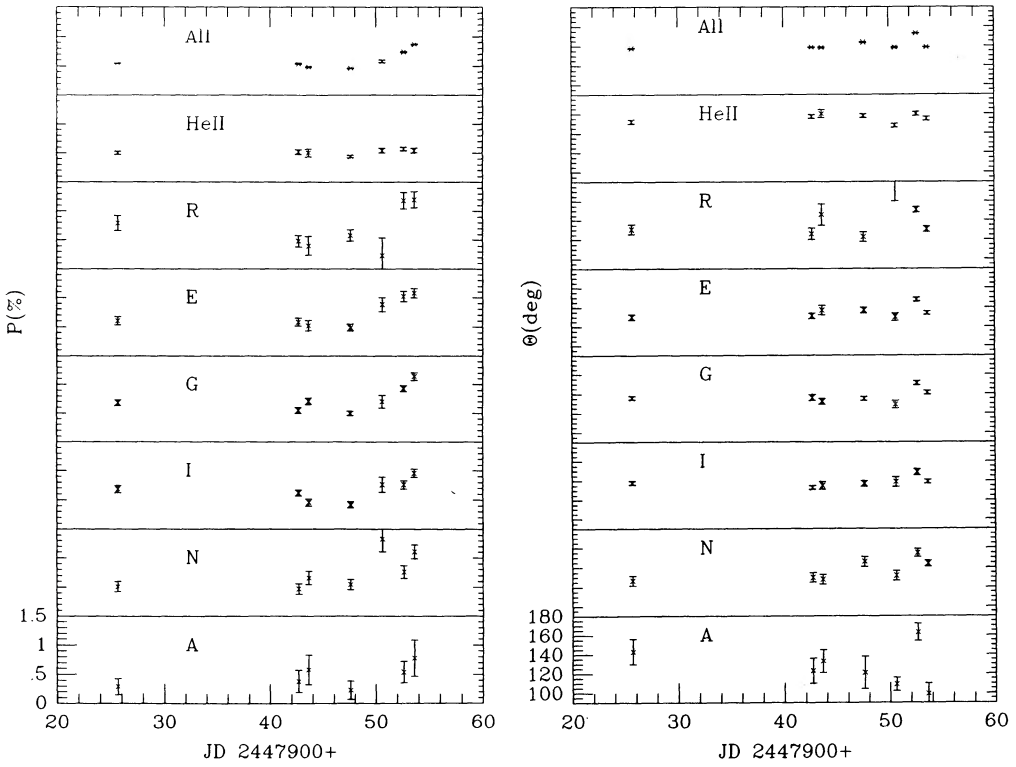

FIG. 4.—Percentage polarization and position angle as a function of time for the integrated polarization and position angle as a function of time for the integrated polarization, He II λ4686, and line-free continuum filters R–A.

tion and position angle in these filters as a function of time for the 1990 data. Also included are the integrated polarization values (3200–7800 Å) and the polarization at He II (4683–4707 Å). We can see from Figure 4 that the integrated percentage polarization changed significantly with time, and increased systematically over the last nights of observation. Whereas the polarization at He II remained relatively constant, the continuum filters followed well the behavior of the integrated polarization. The polarization at He II and in the red (A filter) were smaller than the polarizations in the blue filters. The position angle in the integrated filter displayed significant changes as well; these were traced again by the continuum filters. The position angles in the continuum filters assumed generally lower values than the integrated polarization. The position angle at He II was larger than the continuum values, and the time variability was similar to that of the continuum.

In time-dependent spectropolarimetry, we have to illustrate and interpret a four-dimensional data set, the Stokes parameters Q and U (or both P and Θ) as a function of wavelength and time. When the interstellar polarization is unknown, a method widely used to display the wavelength dependence of the polarization is the plotting of Q and U against each other in a so-called QU diagram. Each point in the QU diagram corresponds to the tip of a vector, given by its Q and U values. A color vector in the QU-plane is a vector that joins a QU pair of a given wavelength with the QU pair of another wavelength, at a given epoch. In connecting all the QU points in order of increasing wavelength, a specific color path is traced in the QU diagram. Over the relatively small wavelength range included in our spectropolarimetry, it may be anticipated that the interstellar polarization does not have much wavelength dependence. It can then, to first order, be visualized as a constant vector; a point in the QU diagram that does not change with wavelength or time which redefines the true zero point of the diagram. The color paths for each observing night, including also the 1989 data set, are shown in Figure 5, where the blue end of a color path is indicated by a larger dot. It can be seen that both the amount and the position angle of the intrinsic polarization in EZ CMa vary as a function of time. The polarizations in 1989 and during the five nights in 1990 February were similar, in position angle and wavelength dependence. Although with some scatter, the polarizations could almost be approximated by a single point in the QU diagram, to within the errors. This indicates that the amount and direction of polarization of EZ CMa have a preferred value. Also, since the polarization was constant as a function of wavelength, we conclude that the dominant polarizing mechanism at these times was electron scattering and that the product of electron density/geometry and aspect angle has a favored combination of parameters as a function of time.

To illustrate the above point further, we have overplotted the color paths of all nights in a single QU diagram; the result is shown in Figure 6. We can see that all nights except for the night of 1990 March 2 are very clustered. There is some small variability even for the quasi-constant nights that becomes discernible on looking only at the large dots. These large dots define a time path traced within a narrow band in Q and U (excepting 1990 March 2). The time path indicates that the position angle of the intrinsic polarization is more confined than the amount of the polarization. This suggests the presence of a preferred axis or symmetry plane in the star/envelope geometry. There appears to be an average physical state that the system assumes, a quasi-static, electron-scattering envelope, which is localized in the star/wind coordinate system and has axial symmetry and a fixed aspect angle to the line of sight.

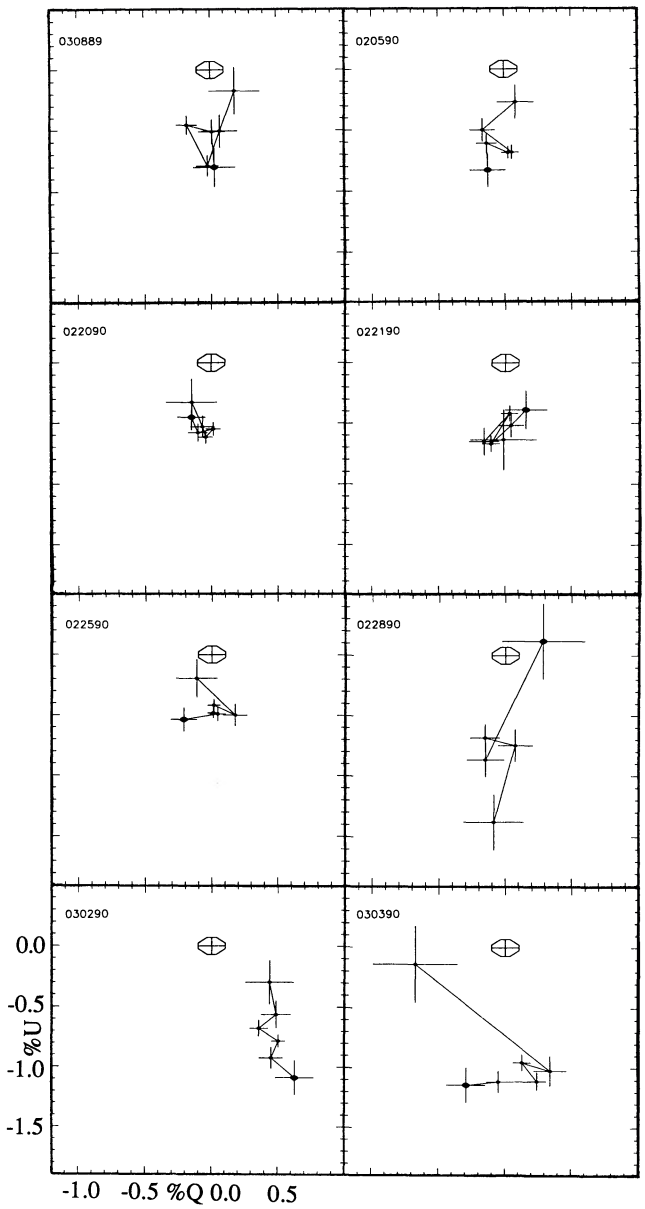

FIG. 5.—QU diagrams for the continuum polarizations as a function of time. The open octahedron indicates the zero point of the diagram.

The polarization and position angle changed significantly during two consecutive nights in 1990 March. The polarization for the night of 1990 March 2 is farthest away from the location defined by the previous nights, while the polarization on 1990 March 3 seems to be swinging back to this location in position angle, but has a higher average amount of polarization. Furthermore, during the night of 1990 March 2, there is a clear trend of polarization with wavelength; the intrinsic polarization has developed color. For the night of 1990 March 3, the error bar is very large for the red-most filter, so that a systematic color behavior is hard to discern. We can conclude that for at least one night of observations, a significant change of the intrinsic continuum polarization was accompanied by a

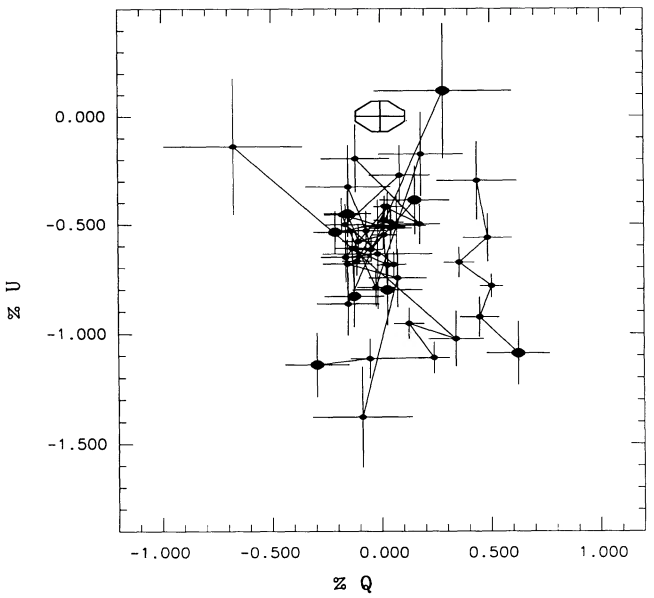

FIG. 6.—QU diagram of all continuum polarizations overplotted. The open octahedron indicates the zero point of the diagram.

change in the spectrum of the polarization. The exact color dependence cannot be determined without knowledge of the interstellar polarization. However, since the amount of polarization changed while the color appeared, it is a concise interpretation that this night indicates a large change in the average electron density in the wind, because an increase in the distribution integral over n_e may be expected to have a pronounced effect on the integral over n_e^2.

The change in the electron distribution integral observed on 1990 March 2 and 3 either may have affected the whole wind around EZ CMa or may have occurred in a confined volume within the wind. Since the position angle of the continuum for the March 2 observation varied along with the amount and color of polarization, we infer that the electron density contrast associated with this event did not have the same shape integral assumed by the quasi-static star/wind electron density distribution. For example, it cannot have been a symmetrical shell ejection into that previously defined geometry. More likely the material formed a confined blob or plume resulting in a sidedness. In this way, even axial symmetry may have been temporarily violated, and a new position angle could have been assumed in the spatial integration over the envelope as the ejected material dominated over the quasi-static component.

We note that the position-angle rotation of the continuum polarization from the February nights to 1990 March 2 and 3 is in the clockwise direction. This is also the sense of rotation deduced in Paper I from the polarization changes across He II λ4686. Therefore, it would appear to be a concise interpretation that the high-density material was injected with a sidedness into the axisymmetric wind geometry, being carried around through rotation before it dissipated. In pursuit of this idea, we further notice that the material should have had an asymmetrical distribution with respect to the major plane of the axisymmetric, rotating envelope, to allow for first harmonic variations in the time dependence of the polarization to occur. Dense plumes ejected at various inclinations into the rotating envelope then present a possible explanation for the quasi-periodic polarization behavior, and might produce both first and second harmonic variability, or none at all when activity pauses.

The time path must intersect with the polarization vector at some value that may occur outside the range traced by the observed variability but along the vector defined by it, i.e., the value where the intrinsic polarization would be zero. Also, the QU vectors for 1990 March 2 are always composed of two vectors of unknown length, intrinsic and interstellar polarization, at a given wavelength. Following Serkowski's law, the interstellar polarization has a maximum at optical wavelengths and tapers off into the far-infrared and ultraviolet, so that at some wavelength the interstellar contribution will be minimized. Both conditions can be satisfied if the interstellar polarization is located at the convergence point of the time path and the 030290 wavelength path. The likely interstellar polarization vector is inferred to have a small positive component in the Q-direction, and to be close to zero in U. We can conclude that the amount of intrinsic polarization has a value of at least several tenths of a percent.

For a spherically symmetric geometry, the shape factor in equation (1) is $\frac{1}{3}$, so that the residual polarization becomes zero. From the observation of the residual polarization, the oblate and prolate cases cannot be distinguished, because a prolate one will appear the same as an oblate one rotated by 90° on the sky. However, for optimum inclination, $i = 90°$, and in the optically thin limit, $\tau \leq 1$, justified by the lack of polarization color in most of our polarization spectra, we can derive an upper limit for γ (lower limit for the flattening), from

$$\gamma \leq \tfrac{1}{3}(1 - P_R/2) \qquad (11)$$

(see Brown & MacLean 1977). The intrinsic polarization as determined from Figure 6 with the new zero point is between about 0.5% and 1%, say 0.75%, and we calculate a shape factor of 0.2. For the ellipsoidal shell model with uniform density of Brown & McLean, this implies a ratio of the equatorial to polar radius $a \geq 5$. The shape of the EZ CMa envelope deviates, on the average, by at least 60% from spherical geometry.

Second, we can also infer the wavelength dependence of the polarization on 1990 March 2. As the interstellar polarization vector has been shown to most likely point to the red end of the color path, it follows that the intrinsic polarization must rise from the red to the blue. While the exact spectrum has to be determined by subtracting the interstellar polarization correctly, the steep rise qualitatively implies that the plume or clump may have had a higher absorptive opacity in the continuum than the quasi-static envelope. This is again consistent with attributing the observed variation to an increase in electron density.

The prominent emission lines are identified in Figure 7*a*. We proceeded to integrate our 1990 data in time, in order to increase the spectropolarimetric signal-to-noise ratio in the weaker lines. For each of the lines, we defined ~30 Å wide bandpasses centered on the observed line centers. The observed polarization of each line itself was then computed by a formal subtraction of the Stokes parameters of the underlying continuum, using a linear interpolation between continuum points defined to the left and the right of the line. The results are presented in Table 2, and in the QU diagram in Figure 7*b*. The continuum filters are connected in wavelength as before. The polarization in the lines is generally smaller than the polarization in the continuum. The line polarization traces a path extending from a bulk of small line polarizations quite

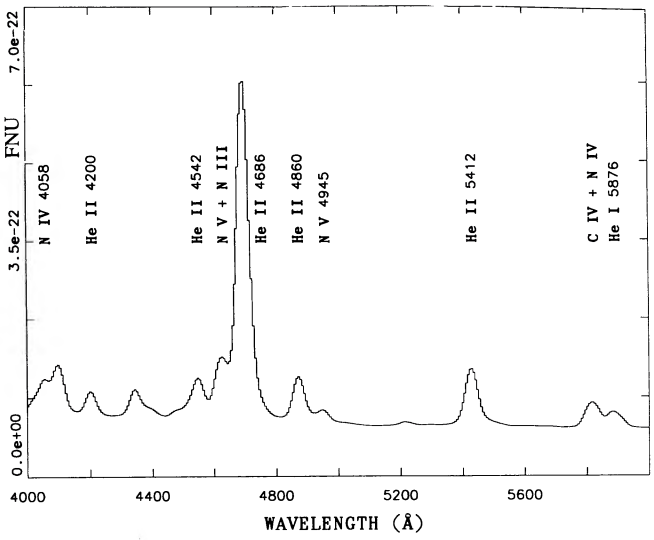

FIG. 7a

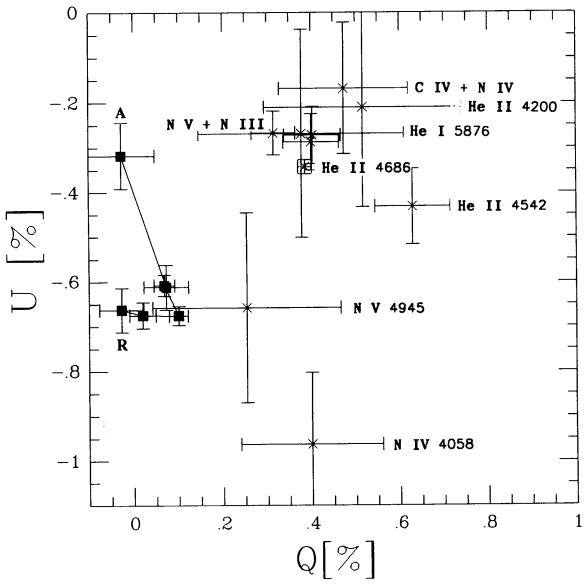

FIG. 7b

FIG. 7.—(*a*) Spectrum with line identifications. (*b*) *QU* diagram of the line polarizations (*crosses*) and continuum-filter polarizations (*filled squares*).

far from the continuum, to a polarization in N v λ4945 that is quite close to the continuum values, to the continuum polarization. If all the lines were unpolarized, they should all assume the same line polarization (to first order), corresponding to the interstellar polarization at the wavelength of the line (neglecting the small wavelength dependence of the interstellar polarization across our spectral range). We infer that the envelope is stratified. Within the error bars, the polarization in the lines has the same direction as the polarization in the continuum. This band of points indicates that we can consider a common polarizing mechanism for both the lines and the continuum, and that the lines see the same geometry as the continuum photons. We note that a possible exception is N IV λ4058, which may have an angle and thus a geometry that differ from the other lines observed here. However, the errors are quite large. The strong polarization in He II λ4686 is persistent, since it was also present on the 1978 and 1979 data of McLean.

TABLE 2

STOKES PARAMETERS FOR VARIOUS FILTERS

Filter	*Q* (%)	*U* (%)	Error (%)
R	−0.027	−0.663	0.049
E	0.020	−0.675	0.029
G	0.100	−0.676	0.021
I	0.068	−0.608	0.023
N	0.072	−0.612	0.050
A	−0.027	−0.318	0.074
He I λ5876	0.378	−0.269	0.232
He II λ4200	0.517	−0.210	0.223
He II λ4542	0.629	−0.432	0.085
He II λ4686	0.386	−0.343	0.016
He II λ4860	0.403	−0.272	0.064
He II λ5412	0.400	−0.287	0.063
N IV λ4058	0.400	−0.963	0.160
N V λ4945	0.254	−0.658	0.212
N V + N III	0.315	−0.267	0.049
C IV + N IV	0.474	−0.168	0.146

We have neglected the time dependence of the polarization. Only the He II λ4686 line is strong enough that we get a good signal-to-noise ratio in the polarization for each individual night. In Figure 8 we display a *QU* diagram of the line polarization and the polarization of the underlying continuum for the 1989 and 1990 data. For each night, the continuum and corresponding line are joined by a color vector. All vectors converge to one direction, the interstellar polarization direction. This shows that the line and continuum see the same geometry for each night. We can then always express the line polarization as a fraction of the continuum polarization. The line either is totally unpolarized or assumes a small amount of polarization. For each observed vector, continuum (*C*), and line (*L*), we may write, using equation (9),

$$Q_{C,\text{observed}} = Q_{C,\text{interstellar}} + Q_{C,\text{intrinsic}}\,, \tag{12}$$

$$Q_{L,\text{observed}} = Q_{L,\text{interstellar}} + Q_{L,\text{intrinsic}}\,, \tag{13}$$

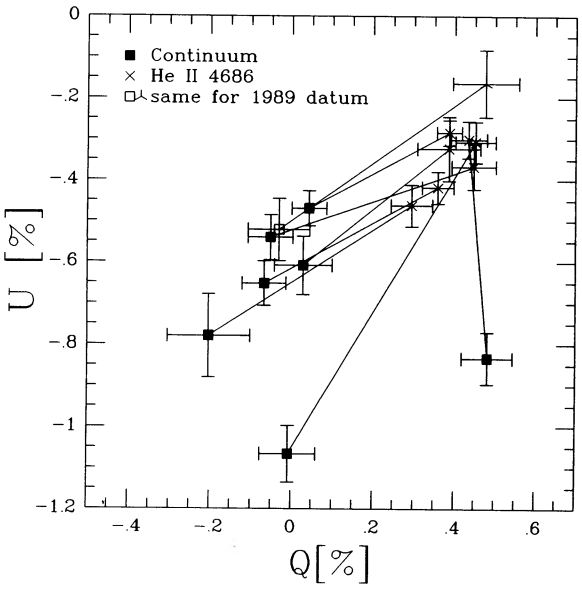

FIG. 8.—He II λ4686 polarization color vectors

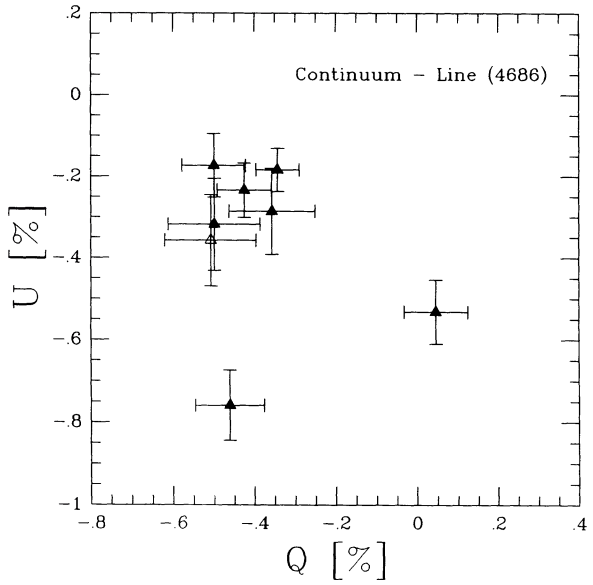

FIG. 9.—QU diagram of continuum minus line polarization at 4686 Å. The open symbol indicates the 1989 datum.

and the same for U using equation (10). Because the line and continuum are measured at the same wavelength,

$$Q_{C,\text{interstellar}} = Q_{L,\text{interstellar}} , \quad (14)$$

the interstellar polarization drops out of the combined equations

$$Q_{C,\text{observed}} - Q_{L,\text{observed}} = Q_{C,\text{intrinsic}} - Q_{L,\text{intrinsic}} , \quad (15)$$

and we can derive the intrinsic polarization at 4686 Å without knowing the interstellar polarization. A QU plot of the continuum minus line polarization is given in Figure 9. By assuming that the strong continuum polarization dominates the result, this figure substantiates further the conclusion drawn from Figure 5 using observed continuum polarization.

3.2. *Inferences from the Intrinsic Polarization*

It is always difficult to determine the interstellar polarization, and a wrong interstellar polarization subtraction will significantly change the results and their interpretation. We will now try to estimate the most likely value of the interstellar polarization, and rediscuss the EZ CMa data after the correction has been applied. The general properties of interstellar polarization were recently reviewed by Clayton & Cardelli (1988).

In Paper I we eliminated from the data an interstellar foreground polarization determined from simultaneous fits of a Serkowski-type law to the continuum polarization of all 1990 nights (where only He II λ4686 had been removed from the polarization spectrum) and the direction of the He II λ4686 line polarization. The parameters were $P_{\max} = 0.55\%$ ($\lambda_{\max} = 5500$ Å) at a position angle of 0°. It was not too critical, for the discussion of the He II line-wing polarization, that the interstellar polarization was very well determined. The above values are now reexamined.

We showed in Figure 7 that the envelope is stratified. Some emission line might be formed far enough out in the wind that its residual line polarization is close to zero. If we take the minimum of all line polarization values from Figure 7*b*, we obtain an upper limit of $Q = 0.5\%$, $U = -0.2\%$ for the interstellar polarization.

However, even the lines with the smallest electron-scattering optical depths might be too polarized to justify this approach. We have shown that the line polarization in He II λ4686 can be expressed as a fraction of the continuum polarization at that wavelength. We can then look for the convergence point of all color vectors in Figure 8, which should be the value of the interstellar vector at that wavelength. The QU parameters of the best convergence point agree extremely well with the above result.

It remains to be seen whether this result also agrees with the (line-free) continuum polarization. The above values are in agreement with the solution suggested for the time path and the wavelength path of Figure 6.

A routine was developed by Nordsieck to estimate the interstellar polarization from multiple observations of a star. The routine assumes that the position angle of the intrinsic polarization does not vary with wavelength, justifiable for EZ CMa from Figure 5 owing to the collinear pattern of QU vectors at a given epoch, and that the interstellar component is constant with time and can be described by the empirical Serkowski law in its updated form given by Wilking, Lebofsky, & Rieke (1982). It then attempts to fit the same interstellar polarization to all observed polarizations, by minimizing the sum of the squares of the deviations. In this way, the routine always tries to ascribe the largest contribution to the observed polarization to interstellar polarization. We need some first-guess parameters to start the iteration. By allowing the Stokes parameters to be the ones derived above, and at the wavelength of He II λ4686, the fit returned these exact same input values, but with large error bars, for the continuum (1989 and 1990 data). However, it is not expected that the maximum polarization occurs shortward of 5000 Å, since this would imply a peculiar reddening behavior owing to the relation

$$R_V = (5.6 \pm 0.3)\lambda_{\max}\,[\mu\text{m}] , \quad (16)$$

where R_V denotes the ratio of total to selective extinction. A value of 5500–5600 Å is in accordance with the average behavior of the interstellar medium, i.e., $R_V = 3.1$. Since we have no good indication observationally as to the $\lambda_{\max}$ that should be chosen for EZ CMa, we have resumed the fitting process, forcing the interstellar polarization to assume its maximum at 5600 Å. In this way, we make no assumptions about the specific line of sight to EZ CMa. It turned out that this process significantly reduced the errors that resulted from the fit at the line wavelength. The result is a $P_{\max}$ of 0.58% (±0.08%), with a position angle of 176°(±4°). This value agrees extremely well with our crude estimate of the interstellar polarization from Paper I, and is also consistent with the line polarizations. Owing to the relation

$$P_{\max}(\%) \leq 9.0E_{B-B}\,(\text{mag}) , \quad (17)$$

we implicitly set a lower limit on the reddening of ~0.06 mag.

Another often-used method to derive the interstellar polarization is by looking at neighboring stars that show no intrinsic polarization. This approach was chosen by McLean et al. (1979), and they derived an interstellar polarization of 0.25% at a position angle of 35°. The result is significantly different from ours, and we have therefore also reexamined the polarization of neighboring stars. Meade has compiled a data base from various published polarization catalogs for use by the Wiscon-

TABLE 3

POLARIZATION OF FIELD STARS

ID/HD	P	P.A.	$m - M$
50093	0.16%	33°.2	7
50877	0.05	65.0	8
51630	0.19	59.5	10
52437	0.16	81.6	8
52812	0.88	39	8
53138	0.35	16	9
54224	0.27	40.1	9
54309	0.65	0.6	7
−27°3748	0.27	111.2	12
54605	0.15	30	9

sin Ultraviolet Photo-Polarimeter Experiment team. Only four stars could be found in a circle of 2° radius and with appreciable distances, $m - M \geq 7$. If the radius was extended to 5°, it included 10 stars. The data are given in Table 3. The polarization is not well organized in the direction toward EZ CMa. The average of neighboring stars is $Q = 0.09\%$ (0.24%) and $U = 0.17\%$ (0.26%), or a percentage polarization of 0.19% at a position angle of 31°. The result agrees reasonably well with McLean's estimate, but not with our internal estimate from EZ CMa spectropolarimetry. Trying to give this value to our fitting routine as a starting guess results in a polarization that swings toward our estimate, but the errors are much larger than before. We conclude that only better line-of-sight polarimetry will be able to settle this issue. The internally derived values will be used throughout this paper.

We removed the interstellar polarization from the observed polarization. One test that can be applied to the result is to compare the position angles of the intrinsic polarization derived after the interstellar was removed with the position angles derived without knowledge of the interstellar polarization. The former value is given by the removal software and corresponds to a mean intrinsic angle of the line-free continuum polarization. The latter position angle was determined from our knowledge that the polarization in He II λ4686 can always be expressed as a fraction of the continuum polarization at 4686 Å. We may then infer the intrinsic position angle in the star/envelope from

$$\tan 2\Theta_{\text{intrinsic}} = (U_{C,\text{observed}} - U_{L,\text{observed}})/(Q_{C,\text{observed}} - Q_{L,\text{observed}}) . \quad (18)$$

The two results are compared in Figure 10. The agreement is fairly good.

In Figure 11 we plotted the intrinsic continuum polarization and position angle for each observing night (1989 and 1990). It can be seen that the level of continuum polarization is indeed high, as previously claimed. Such a high continuum polarization requires pronounced deviation from spherical symmetry and an inclination that is far from pole-on. The position-angle wavelength dependence is flat, within the error bars, and the level changes by about 30°. The wavelength dependence of the residual polarization is flat, to within the error bars, as expected from pure, thin electron scattering. An exception is presented by the 1990 March 2 data, which demonstrate a clear trend of rising polarization into the UV.

To better illustrate the difference in the polarization spectra, we have compared in Figure 12 the intrinsic continuum polarization of our best signal-to-noise night, 1990 February 25, and

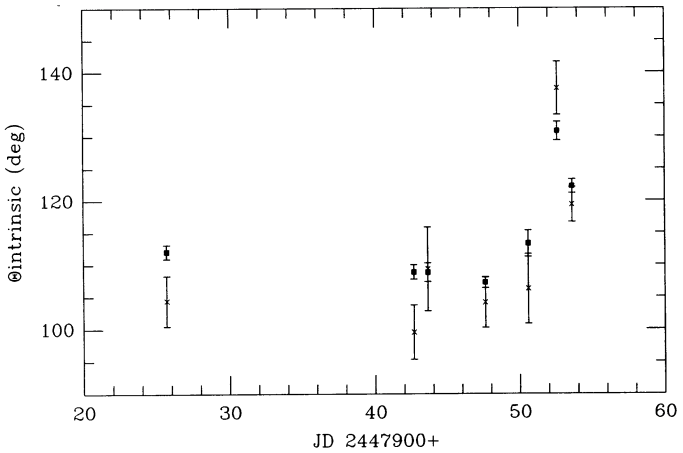

FIG. 10.—Comparison of intrinsic position angles from observed 4686 Å polarization (*crosses*) and integrated polarization after using interstellar-polarization removal software (*filled squares*).

that of 1990 March 2. It can be clearly seen that the color of 1990 March 2 rises from the red into the blue. The polarization cannot be due to Thomson scattering alone. Instead, such wavelength dependence is anticipated if continuum absorption has come to play a role, e.g., in a dense and cool plume, and we will refer to this night as the one displaying the absorption event.

We note that Doherty (1990) has run preliminary ellipsoidal shell models for rotating stars with an optical depth (at 1500 Å) in the equator 5 times larger than in the polar direction. He finds that the polarization color of the absorption event in EZ CMa can be reproduced for an equatorial optical depth as low as unity. The effect of large optical depth, i.e., multiple scattering, has recently been under investigation by Whitney & Code (1989). Using Monte Carlo calculations, they showed that while being reduced by absorption the polarization is still appreciable even for optical depths of 100 in a disk geometry.

With the interstellar polarization removed, the mean intrinsic polarization of all nights becomes 0.77% at a position angle of 109°. The amount of intrinsic polarization is fairly close to our initial estimate, and requires a large deviation from spherical symmetry for an optically thin ellipsoidal shell of uniform electron density (see eq. [11]). The amplitude of the polarization variability is 0.39%. The observed polarization changes can be explained by a ~50% variation in electron density. This is quite a lot. If we exclude the last night of observation, assuming that it might be influenced by the absorption event, and look instead at the amplitude of variability in the "pure scattering" nights, the result is 0.29%, or a density change of 38%.

The polarized intensity at the line wavelengths can be expressed as the sum of the polarized intensities in the continuum and the lines:

$$I_T Q_T = I_C Q_C + I_L Q_L \quad (19)$$

(and the same for U). For an unpolarized line that is very strong, one can make the assumptions that $Q_L = 0$ and $I_L/I_C \gg 1$. Equation (19) then reduces to

$$Q_T/Q_C = 1/(I_L/I_C) . \quad (20)$$

This relation states that the intrinsic continuum polarization at the line wavelengths is inversely proportional to the line-to-

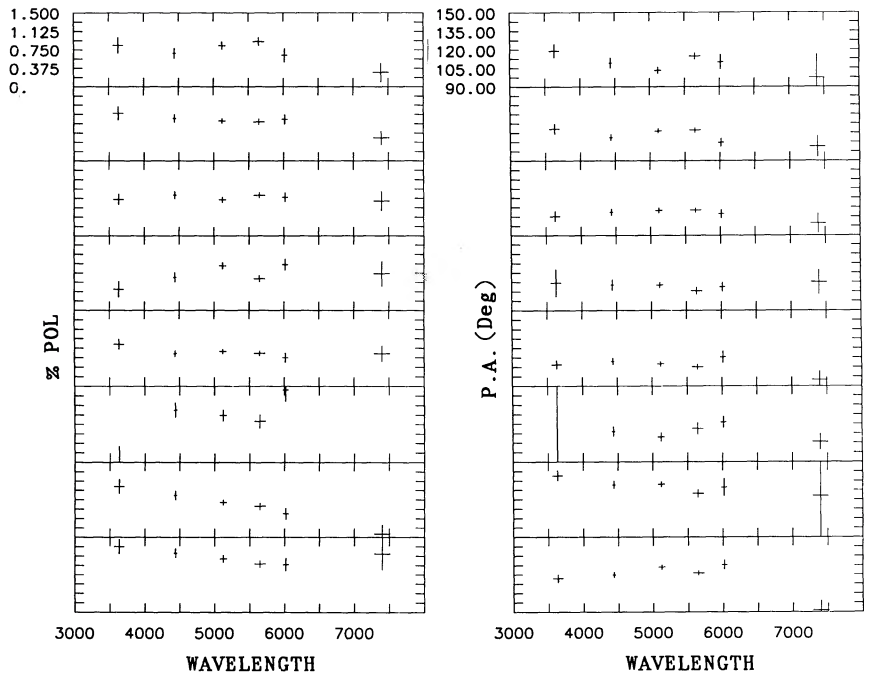

FIG. 11.—Spectra of intrinsic continuum polarization and position angle in the line-free continuum bandpasses, in temporal sequence

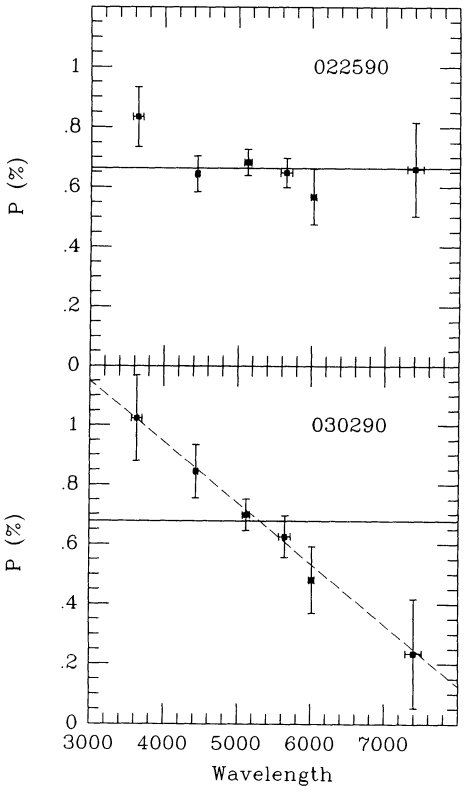

FIG. 12.—The shape of most intrinsic polarization spectra is flat, exemplified by the continuum data of 1990 February 25. The solid horizontal line represents the mean. On 1990 March 2 the polarization rose into the UV. The dashed line fits the data much better than the sold line. There are no significant discontinuities apparent in the data.

continuum intensity ratio, i.e., the continuum will suffer depolarization at the line wavelengths due to dilution (without changes in position angle). Equation (20) was used by McLean et al. (1979) in their discussion of the stratification in the EZ CMa envelope (see their Fig. 3). If we make no assumptions about the emission lines, we may instead write

$$Q_L/Q_C = [(Q_T/Q_C)(1 + I_L/I_C) - 1]/(I_L/I_C) \qquad (21)$$

(and the same for U). In fact, it is exactly this equation which we used to separate the line and continuum polarizations in our measurements. We will also use the line and continuum polarizations rather than the continuum polarization at the line wavelength to investigate whether the line emission is in itself partially polarized as a result of subsequent electron scattering. As can be seen from equation (21), in this normalization an unpolarized emission line assumes a value of zero, while a line as polarized as the continuum is described by a value of unity.

We have measured the Stokes parameters in our combined data set of EZ CMa. Table 4 lists the ratios of Q_L/Q_C and

TABLE 4

INTRINSIC LINE POLARIZATIONS

Filter	Q_I/Q_C	$d(Q_I/Q_C)$	U_I/U_C	$d(U_I/U_C)$
He I λ5876	0.39	0.46	0.35	0.45
He II λ4200	0.14	0.44	0.20	0.37
He II λ4542	−0.14	0.17	0.60	0.15
He II λ4686	0.34	0.03	0.44	0.03
He II λ4860	0.34	0.13	0.32	0.11
He II λ5412	0.36	0.13	0.36	0.12
N IV λ4058	0.30	0.31	1.49	0.29
N V λ4945	0.69	0.43	0.96	0.37
N V + N III	0.48	0.10	0.31	0.09
C IV + N IV	0.20	0.29	0.15	0.28

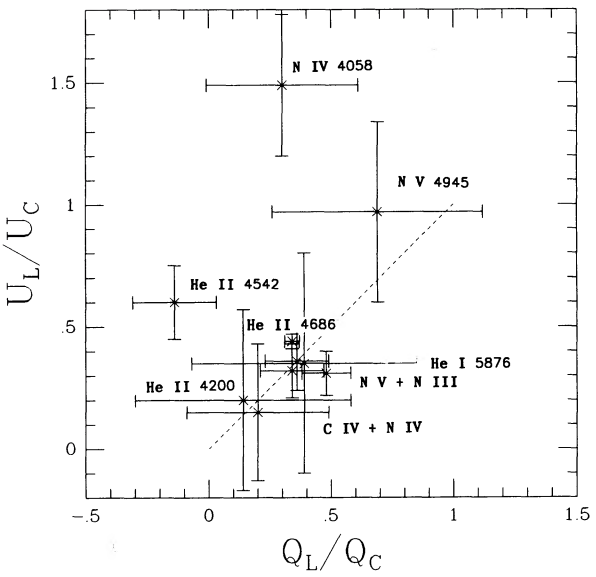

FIG. 13.—Diagnostic diagram for atmospheric stratification. In this normalization, the continuum polarization is unity, and an unpolarized emission line has a polarization of zero. The dashed line represents fractional polarizations at the same position angle as the continuum polarization.

U_L/U_C for the emission lines. These data are plotted against each other in Figure 13.

We can see from Figure 13 that the emission lines in EZ CMa all exhibit some amount of polarization. This indicates that the line photons are being electron-scattered. Almost all lines fall along the 45° line, implying that the line-forming regions have the same geometry as the continuum. Finally (and in spite of the large error bars), we can also notice that the emission lines N IV λ4058 and N V λ4945 display a much larger polarization than the bulk of He II lines and He I λ5876. This is in agreement with an outward decrease of ionization in the wind.

Hillier (1987a, b, 1988) conducted a detailed theoretical investigation into the stratification structure of the EZ CMa wind. He predicts the radius/electron density ranges for an appreciable number of He, N, and C line-emitting regions. Ordering the lines by mean densities (and assuming a nonspherical geometry to produce polarization, respectively), one would indeed predict from Hillier's models that the nitrogen lines should display the largest line polarizations, while that of He II λ4686 is anticipated to be rather small. He I λ5876 should contain the fewest electron-scattered line photons of any line in the optical spectrum. This is confirmed by our observations. However, the He II Pickering lines, originating at medium to high densities in Hillier's models, are expected to be found at comparatively higher polarizations than those of He II λ4686 and He I λ5876, contrary to our observations. Thus, while our data lend some support to the idea of ionization stratification, there are also discrepancies. A better understanding of the envelope stratification of EZ CMa will require both higher signal-to-noise polarimetric measurements and polarization to be included in the empirical envelope models.

4. CONCLUSIONS

We summarize our findings in the following statements:

1. The wind of EZ CMa is not spherically symmetric, as indicated by a large amount of intrinsic continuum polarization.
2. The polarization is due to electron scattering, since the spectrum of the continuum polarization is flat at most epochs.
3. The spectrum of the continuum polarization may rise into the UV at some epochs. This spectral shape can be understood through frequency-dependent absorptive opacity in the helium continuum.
4. The continuum polarization has a large, quasi-static component that can be explained with an inclined-disk model. This geometry extends rather far into the wind, since it is seen also by line-forming regions.
5. We attribute polarization variations to changes in wind density rather than wind geometry, e.g., due to binarity. Periodic variations may be driven by rotation; in combination with density changes, both first and second harmonic variability can arise as a function of time.
6. The optical emission lines are polarized, which implies that the line photons are being electron-scattered.
7. The line polarizations give observational evidence of ionization stratification in the EZ CMa wind.

Pine Bluff Observatory is a team effort. We are grateful to the people who support this installation, and to the dedicated observers. We would like to thank M. R. Meade and B. L. Babler for their excellent assistance in the data reduction. R. S.-L. acknowledges the many interesting discussions with A. D. Code on extended atmospheres. This work was supported by NASA contract NAS5-26777 to the Wisconsin Ultraviolet Photo-Polarimeter Experiment.

REFERENCES

Beals, C. S. 1929, MNRAS, 90, 202
Brown, J. C., & McLean, I. S. 1977, A&A, 57, 141
Brown, J. C., McLean, I. S., & Emslie, A. G. 1978, A&A, 68, 415
Cassinelli, J. P., & Castor, J. I. 1973, ApJ, 179, 189
Cassinelli, J. P., & Hummer, D. G. 1971, MNRAS, 153, 9
Cassinelli, J. P., Nordsieck, K. H., & Murison, M. A. 1987, ApJ, 317, 290
Clayton, G. C., & Cardelli, J. A. 1988, AJ, 96, 695
Doherty, L. R. 1990, private communication
Drissen, L., Robert, C., Lamontagne, R., Moffat, A. F. J., St.-Louis, N., van Weeren, N., & van Genderen, A. M. 1989, ApJ, 343, 426
Firmani, C., Koenigsberger, G., Bisiacchi, G. F., Moffat, A. F. J., & Isserstedt, J. 1980, ApJ, 239, 607
Hamann, W.-R., Schmutz, W., & Wessolowski, U. 1988, A&A, 194, 190
Hillier, D. J. 1987a, ApJS, 63, 947
———. 1987b, ApJS, 63, 965
———. 1988, ApJ, 327, 822
Lamongtagne, R., Moffat, A. F. J., & Lamarre, A. 1986, AJ, 94, 1008
McLean, I. S. 1980, ApJ, 236, L149
McLean, I. S., Coyne, G. V., Frecker, J. E., & Serkowski, K. 1979, ApJ, 231, L141
Nook, M. A. 1990, Ph.D. thesis, University of Wisconsi–Madison
Nordsieck, K. H. 1987, BAAS, 19, 1098
———. 1991, in preparation
Robert, C., Moffat, A. F. J., Drissen, L., Niemela, V. S., Barrett, P., Seggewiss, W., & Lamontagne, R. 1991, in IAU Symposium 143, Wolf-Rayet Stars and Interrelations with Other Massive Stars in Galaxies, ed. K. A. van der Hucht & B. Hidayat (Dordrecht: Kluwer), 181
Schmutz, W. 1991, in IAU Symposium 143, Wolf-Rayet Stars and Interrelations with Other Massive Stars in Galaxies, ed. K. A. van der Hucht & B. Hidayat (Dordrecht: Kluwer), 39
Schulte-Ladbeck, R. E., Nordsieck, K. H., Nook, M. A., Magalhães, A. M., Taylor, M., Bjorkman, K. S., & Anderson, C. M. 1990, ApJ, 365, L19 (Paper I)
Serkowski, K. 1970, ApJ, 160, 1083
Torres-Dodgen, A. V., & Massey, P. 1988, AJ, 96, 1076
Whitney, B. A., & Code, A. D. 1989, BAAS, 21, 1114
Wilking, B. A., Lebofsky, M. J., & Rieke, G. H. 1982, AJ, 87, 695